J. Appl. Eng. Sci. Technol. (2018) 4(2): 123-128

Numerical study of the active earth pressure distribution on cylindrical shafts using 2D finite difference code

Abdelmadjid Meftah[1,2]✉, Naïma Benmebarek[1], Sadok Benmebarek[1]

1 University of Mohamed Khider Biskra, NMISSI Laboratory, Faculty of Science and Technology, 145 BP RP, 07000, Biskra, Algeria

2 University of Mentouri Brothers, Constantine, 25000, Algeria

Received 28 March 2018

Published online: 11 June 2018

Keywords

Vertical circular shaft

Arching effect

Axisymmetric earth pressure

Numerical modeling

Soil

Interaction

Abstract: The present paper examine the distribution of the active pressure on a circular shaft embedded in granular material subjected to radial displacement. The deformation problem was solved under axisymmetric conditions using explicit finite difference code FLAC (Fast Lagrangian Analyses of Continua). Based on the numerical results, the distribution of the active pressure with increasing excavation depth is non-linear for all interface angle of the shaft, for different diameters and height of the shaft also for the all friction angles of the soil. When friction angle of the soil that are less than, or equal to 10° the active pressure is linear. These results are summarized and compared against previously published theoretical solutions and experimental results.

1. Introduction

One of concerns of the geotechnical domain is the study of soil and its interaction with any type of structures (e.g tunnels, pumping stations and hydroelectric projects) which they are able to support the soil either in a natural state or after treatment.

It is well known that in Civil Engineering, lateral earth pressures that act on retaining walls can be calculated using either Rankine's or Coulomb's theories. Both theories assume that the distribution of lateral earth pressure is triangular. However, this is not a key factor in design of vertical shafts. Because that are not only this is not as close to reality but do not taking into consideration the mode of structural movement.

Much theoretical works has been done to study the lateral earth pressure acting on a rigid wall have been made to extend plane strain active earth pressure methods. For example, (Westergaard 1941) and (Terzaghi 1943) proposed analytical solutions and (Prater 1977) used the limit equilibrium method. In references (Berezantzev 1958 ; Cheng and Hu 2005 ; Cheng et al. 2006 ; Liu and Wang 2008 ; Liu et al. 2008) the slip line method it used. In contrast to the classical earth pressure theories, where the active earth pressure calculated using the Coulomb or Rankine method are essentially the same, the distributions obtained for axisymmetric conditions may differ considerably depending on the chosen method of analysis, as discussed below.

Several experimental investigations have proposed different techniques to measure the changes in lateral earth pressure due to the installation of model shafts in granular material under of each of axisymmetric condition, normal gravity conditions or in a centrifuge (Fujii et al. 1994 ; Herten and Pulsfort 1999 ; Imamura et al. 1999 ; Chun and Shin 2006 ; Tatiana and Mohamed 2011 ; Cho et al. 2015). However, in these studies, there is no general agreement on the radial earth pressure distribution along the shaft.

The objective of this study is to simulate the shaft excavation process in one stage and in four stages for investigate the active earth pressure on cylindrical shaft linings installed in cohesion-less ground and the required displacement for establishing active conditions by numerical approach using the explicit finite difference code FLAC (Fast Lagrangian Analyses of Continua 2005). The results of the numerical studies are then analyzed and conclusions are made regarding the distribution of the radial, tangential and vertical stresses around the shaft as well as the distribution of lateral earth pressure. These results are compared to published experimental results and theoretical solutions.

2. Testing program

The experimental study of the earth pressure distribution on cylindrical shafts reported by (Tobar and Meguid 2011) is numerically investigated by using the computer code FLAC. The soil behavior is modeled by the elastic-perfectly plastic Mohr–Coulomb model encoded in FLAC code. All results in this test are given for γ = 18.00 kN/m^3, elastic bulk modulus K = 30 MPa and shear modulus G = 11.25 MPa, different internal friction angles (φ = 10° and 41°) and cohesion c = 0.

The proposed modeling procedure of the active earth pressure distribution on cylindrical shafts follows two steps:

✉ Corresponding author. E-mail address: meftahbde@hotmail.fr

- In the first one, the shaft installation and the geostatic stresses are computed assuming fixed shaft connected to the soil via interface element. At this stage the strength of the interface elements are assigned to be null and some stepping is required to bring the model to equilibrium.
- In the second step, a radial velocity of 10^{-6} m/step towers the shaft axis was applied to the grid points representing. The wall shaft until a steady plastic flow is achieved (i.e. until a constant pressure on the shaft wall is reached). As the level of errors in such calculation scheme by FLAC depends on the applied velocity, a low velocity is recommended.

The mesh size is fine near to the wall where deformations are concentrated. As a general rule for the boundary conditions, the bottom boundary is assumed to be fixed in the vertical direction, the right and left lateral boundaries are fixed in the horizontal directions. For axi-symmetry problem, structural elements incorporated in FLAC don't work. Therefore, the shaft wall is modeled by thin fixed membrane elements connected to the soil grid via interface elements attached on both sides. Figure 1 show the axi-symmetric mesh retained for this testing analysis and plastic zone corresponding to limit state. Figure 2 shows the numerical results of the active earth pressure distribution with shaft depth for two values of the earth pressure at rest K_o = 0.5 and K_o = 1. The results confirm that variation in practical range of the earth pressure coefficient at rest K_0 do not have any significant influence on the axi-symmetric active earth pressure distribution.

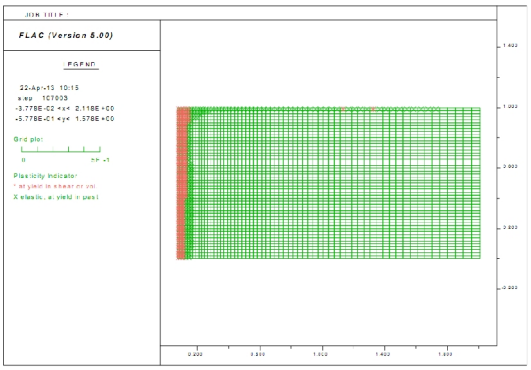

Fig. 1. Mesh used and plastic zone for a rigid vertical shaft.

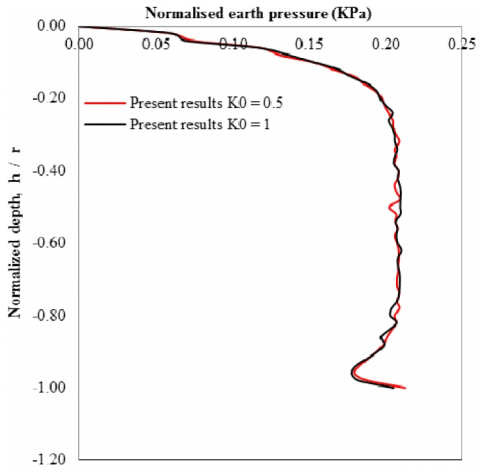

Fig. 2. Active earth pressure distribution.

Figures 3 and 4 show the comparison of present results to theoretical solutions (Terzaghi 1943 ; Prater 1977 ; Berezantzev 1958) and experimental results (Tobar and Meguid 2011), it can be noted that the present numerical results agree well with the measured earth pressure (Tobar and Meguid 2011) and the solutions (Terzaghi 1943 ; Berezantzev 1958). It appears from this comparison that the measured earth pressure decreases with increasing wall displacement until it coincides between (Berezantzev 1958) and Terzaghi's solutions at a wall displacement that corresponds to 0.25% of the wall height.

The radial, tangential and vertical stress distributions in the medium and in radial direction at the half of the model height are plotted in Figures 5, 6, 7 and 8 respectively. The results show a slight increase of the vertical stress (σ_v) in the elastic region near the elastic-plastic interface followed by a drastic reduction in the plastic region. This behavior indicates that arching in vertical planes is formed. The tangential stresses (σ_θ) increase toward the shaft wall in the elastic region, followed by a brutal decrease and converge to vertical stresses in the plastic region. Also, the radial stresses (σ_r) decrease toward the shaft wall accentuated in the plastic zone.

3. Test results and discussion

A numerical study was performed for a physical model to investigate the earth pressure distribution on a cylindrical shaft. The results were compared with both some theoretical solutions and experimental measurements of the physical model.

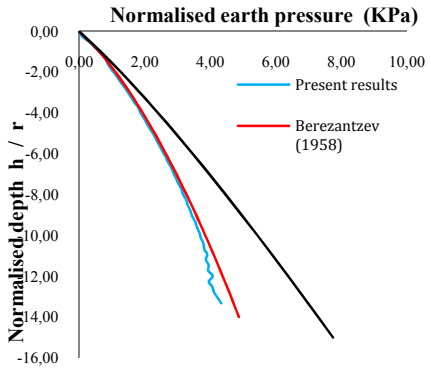

Fig. 3. Comparison of active earth pressure distribution with φ = 10°.

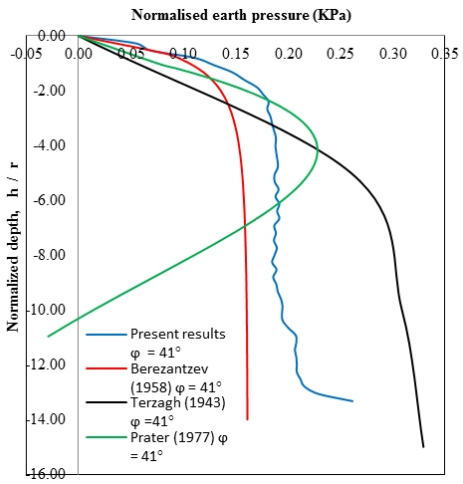

Fig. 4. Comparison of active earth pressure distribution with φ = 41°.

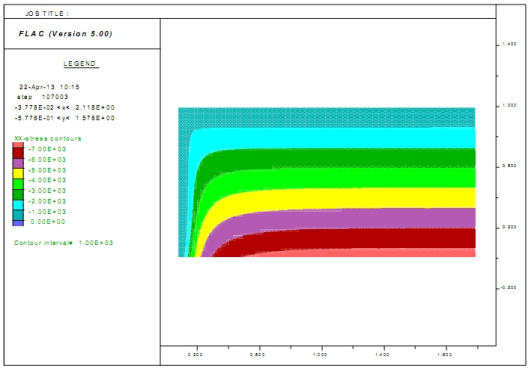

Fig. 5. Distribution of radial stresses (σ_r) at limit state.

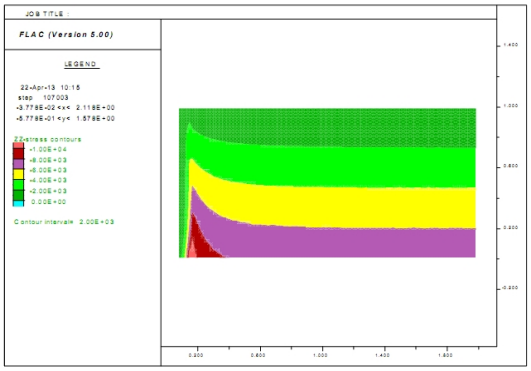

Fig. 6. Distribution of the tangential stresses (σ_θ) at limit state.

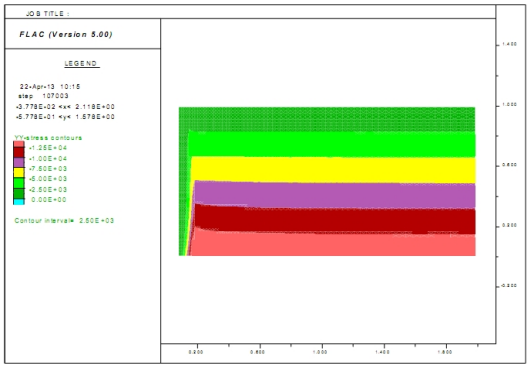

Fig. 7. Distribution of the vertical stresses (σ_v) at limit state.

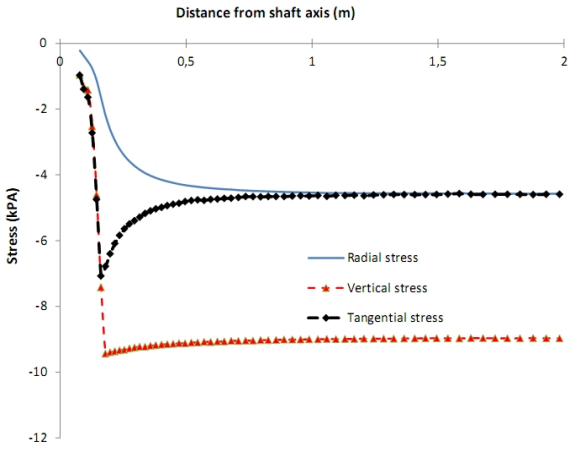

Fig. 8. Stresses distribution at 0.4H from the base.

The numerical, the theoretical and the experimental results show that the axi-symmetric active earth pressure distribution for cylindrical shafts does not increase linearly with depth as it does plane strain conditions.

The wall movement induces a reduction of the earth pressure distribution until a constant value at the ultimate state for high friction soil. The theoretical solutions show high discrepancy related to the hypothesis concerning the lateral stress coefficient $\lambda = \sigma_\theta/\sigma_v$ which cannot be determined from the theories. A good agreement was noted between the present numerical modeling results, experimental results (Tobar and Meguid 2011) and theoretical solutions of (Terzaghi 1943 ; Prater 1977 ; Berezantzev 1958) which both assuming a value of λ equal to unity. FLAC numerical results show a drastic reduction of the vertical stresses (σ_v) and tangential stresses (σ_θ) in the plastic region against the shaft wall and confirm the hypothesis $\lambda = \sigma_\theta/\sigma_v = 1$ assumed by (Terzaghi 1943 ; Prater 1977 ; Berezantzev 1958).

4. Parametric Analysis

Physical model had been used to study the changes in earth pressure distribution due to the next parameters, shaft diameter (D), the shaft height (H), the internal friction angle of the soil (φ), the shaft interface angles (δ) and the staged excavation. The soil behavior is modeled as Mohr-Coulomb material and the modeling procedures are similar to the modeling mentioned in Section 2.

The model has a height exceeds the sum of 0.7H below the level of the shaft toe, plus the height of the vertical shaft (H) and a length of ten times the diameter of the vertical shaft from the center of the shaft. These dimensions were chosen to minimize the boundary effects on the performance of the vertical shaft. The mesh size is fine near the wall where deformations are concentrated and in excavation background using concrete element. All results in this analyses are given for $\gamma = 20.00$ kN/m^3, elastic modulus $E = 7.8 \times 10^7$ Pa and Poisson's ratio $\nu = 0.3$, different internal friction angles (φ = 10°, 20°, 30° and 40°) and cohesion c = 0. Figure 9 shows the axi-symmetric mesh retained for this analysis.

4.1 Effect of shaft diameter

Figure 10 demonstrates the distribution of active lateral earth pressures, with different diameter of the shaft (D = 1.5, 3, 6 and 10 m) for the same height of shaft (h = 3 m).

The present results indicate the reduction of active lateral earth pressures when the diameter of the shaft increases. To illustrate, for large shaft diameters, the distribution of the lateral earth pressure is similar to plane strain conditions. This result is similar to the description of the effect of the shape of drilled shafts provided by (Liang and Zeng 2002).

4.2. Effect of internal friction angle

Figure 11 illustrate the distribution of active lateral earth pressures, with different internal friction angles (φ = 10°, 20°, 30° and 40°) for the same height of shaft (h = 3 m). In this figure the

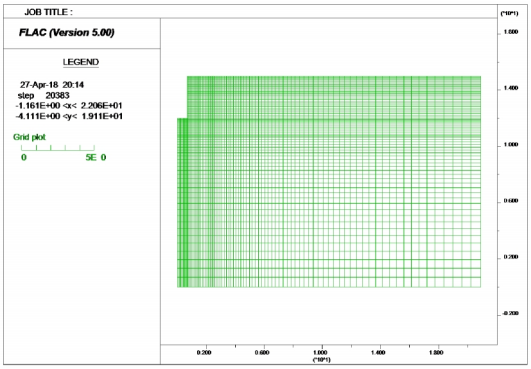

Fig. 9. Mesh used for a rigid vertical shaft (D = 1.5 m).

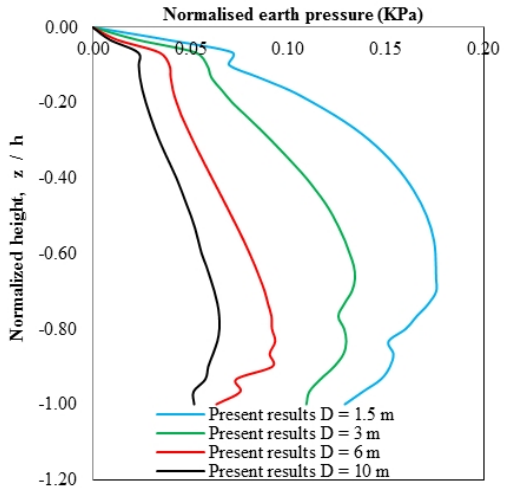

Fig. 10. Effect of shaft diameter (φ = 40° and δ = 0°).

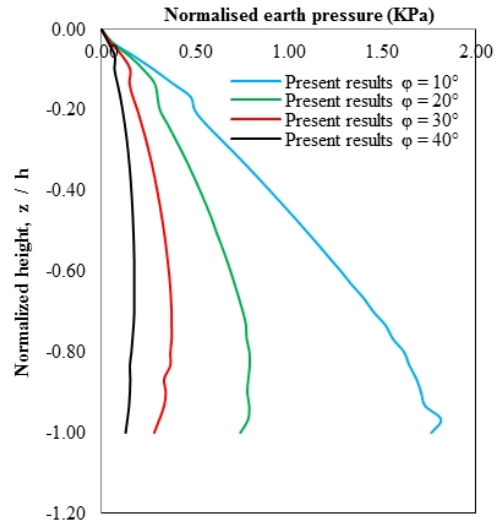

Fig. 11. Effect of internal friction angle of the soil (D = 1.5 m and δ = 0°).

distribution of the active earth pressure calculated using the computer code FLAC 2D is non-linear for all friction angles of the soil except for φ = 10° is linear. We attribute this difference to the reduction in the arching effects due to low frictional between soil grains. The present results indicate the reduction of active lateral earth pressure, with an increase of the internal friction angle of the soil. The results also indicate stronger arching for soil with a higher friction angle.

4.3. Effect of the shaft interface

Figure 12 illustrate the distribution of active lateral earth pressures, with different shaft interface angles (δ = 10°, 20°, 30° and 40°) for the same height of shaft (h = 3 m). The figure 12 indicates the low effect of the shaft interface on the distribution of the active lateral earth pressures, which are similar to the experimental results obtained by (Fujii et al. 1994).

4.4. Effect of the shaft height

Figure 13 represent the distribution of active lateral earth pressures, with different shaft height (H = 3, 6 and 9 m) for the same diameter of shaft (D = 10 m). The results indicate that the distribution of lateral earth pressure is clearly related to the shaft height, and the pressure increases significantly with increasing shaft height.

4.5. Effect of the staged excavation

The experimental study of the earth pressure distribution on cylindrical shafts reported by (Cho et al. 2015) is numerically investigated by using the computer code FLAC. The soil behavior is modeled by the elastic-perfectly plastic Mohr–Coulomb model encoded in FLAC code. The properties of the soil, shaft and interface are summarized in Table 1. The mesh size is fine near the wall where deformations are concentrated. As a general rule for the boundary conditions, the bottom boundary is assumed to be fixed in the vertical direction, the right and left lateral boundaries are fixed in the horizontal directions.

Table 1. Geotechnical parameters of the soil, shaft and interface.

	Shaft	Soil	Interface
γ (Unit weight; kN/m^3)	27	12.60	/
φ (Soil friction angle; °)	/	36.95	26.75
ψ (Dilation angle; °)	/	0	0
c (Cohesion; kN/m^3)	/	4500	3015
E (Elastic modulus; MPa)	72	10	/
ν (Poisson's ratio)	0.2	0.3	/
G (Shear modulus; MPa)	30	3.8	/
K (Elastic bulk modulus; MPa)	40	8.3	/
K_s (Shear stiffness; MPa)	/	/	1470.7
K_n (Normal stiffness; MPa)	/	/	133.7
σ_t (Tensile strength; MPa)	/	0	0

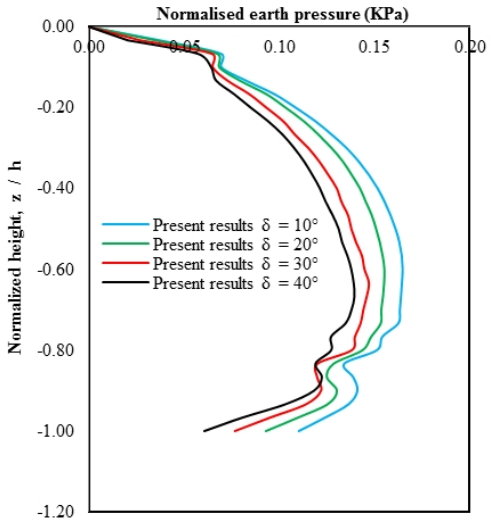

Fig. 12. Effect of shaft interface (D = 1.5 m and φ = 40°).

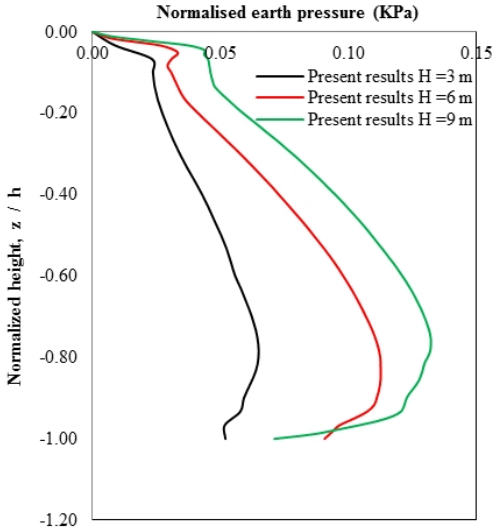

Fig. 13. Effect of the shaft height (D = 10 m and φ = 40°).

Representative result of the finite elements analysis provided by (Cho et al. 2015) and the FD analysis (FLAC 2D) are shown in Figure 14. The results show that the computed lateral earth pressures near the each section of the vertical shaft are slightly less than the experimental results provided by (Cho et al. 2015) because the FD numerical model (i.e., continuum analysis) did not consider the separation between the vertical shaft and the soil that occurred in the experiments, as indicated by (Cho et al. 2015).

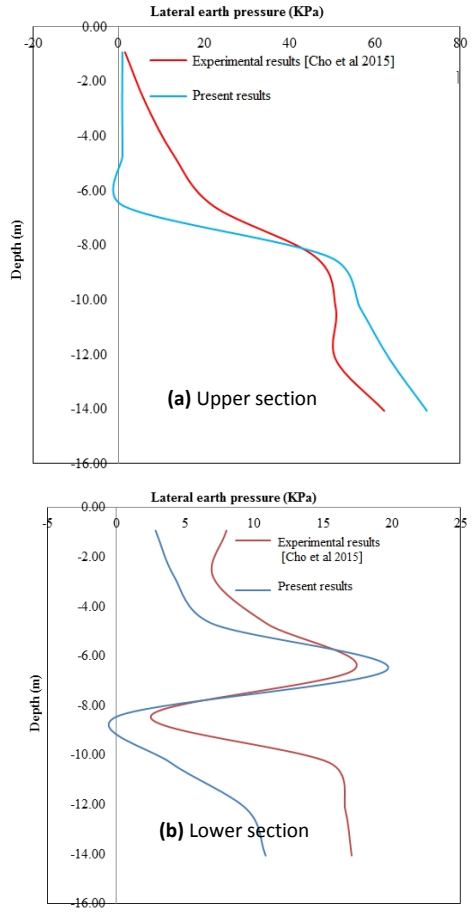

Fig. 14. Comparison of active earth pressure distribution (δ_h/H = 0.2×10^{-2}).

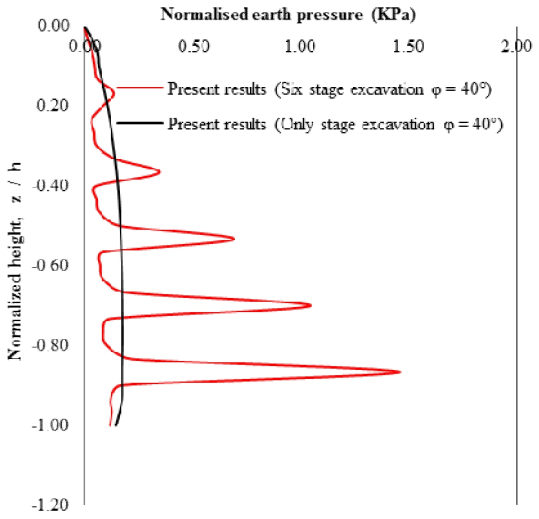

Fig. 15. Effect of the staged excavation.

The excavation by progressively, was being applied onto the model that was adopted in the section (Parametric analysis), the first excavation of the 3 meters has been modeled in steps of 0.50 m in length to simulate a realistic excavation sequence for the vertical circular shaft. To simulate six-stage excavation, the first section was subjected to a homogeneous radial displacement, and is followed by the five excavations then moved in the same manner.

Figure 15 demonstrate the distribution of active lateral earth pressures, with different stage excavation (only stage / six stage) for the same height of shaft (h = 3 m). The present results indicate that the distribution of lateral earth pressure on a vertical circular shaft according to the excavation sequence is non-linear, as found in only stage excavation. It is also observed in each stage of excavation large pressures at the bottom of the excavated shaft.

5. Conclusions

Some existing theories for the prediction of the active earth pressure on the shaft are easy to apply but there is an overestimation of these pressures, namely Coulomb's theory and Rankine's theory. On another side, it can also be observed that Prater, Terzaghi and Berezantzev's methods easy to apply but underestimate the active pressure. However, only the numerical analysis can examine the arching effect. In this computational research investigates the active earth pressure on a circular shaft embedded in granular material subjected to radial displacement using explicit finite difference code FLAC. Based on the obtained numerical results, the internal friction angle has a more significant effect on lateral earth pressure active than the geometry of the vertical shaft (i.e., the diameter, height and interface of the shaft). Also, the results confirm that variation in the shaft interface have any low effect on the axi-symmetric active earth pressure.

FLAC program indicate a drastic reduction of the vertical stress (σ_v) and tangential stresses (σ_θ) in the plastic region against the shaft wall and confirm the hypothesis $\lambda = \sigma_\theta/\sigma_v = 1$. Beside, the

distribution of lateral earth pressure is non-linear in both sequence and each stage of excavation and the arching effect is more significant for high internal friction angles.

References

Benmebarek, S., A. Meftah, N. Benmebarek (2013) Numerical Study of the Earth Pressure Distribution on Cylindrical Shafts, International Symposium on Innovative Technologies in Engineering and Science, Sakarya University Congress and Culture center 283-292.

Berezantzev, V. G. (1958) Earth pressure on the cylindrical retaining walls. In: Conference on Earth Pressure Problems, Brussels 21–27.

Cheng, Y. M., Y. Y. Hu (2005) Active earth pressure on circular shaft lining obtained by simplified slip line solution with general tangential stress coefficient. Chin. J Geotech. Eng. 27(1): 110–115.

Cheng, Y. M., Y. Y. Hu., W. B. Wei (2007) General axisymmetric active earth pressure by method of characteristics – theory and numerical formulation. Int. J. Geomech. 7 (1): 1–15.

Cho J., H. Lim, S. Jeong, K. Kim (2015) Analysis of lateral earth pressure on a vertical circular shaft by considering the 3D arching effect, Tunnelling and Underground Space Technology 48: 11–19.

Chun, B., Y. Shin (2006) Active earth pressure acting on the cylindrical retaining wall of a shaft. South Korea Ground Environ. Eng. J. 7(4): 15–24.

FLAC (2005) Fast Lagrangian Analysis of Continua, ITASCA Consulting Group, Inc, Minneapolis.

Fujii, T., T. Hagiwara., K. Ueno., A. Taguchi (1994) A Experiment and analysis of earth pressure on an axisymmetric shaft in sand. Proc., Int. Conf. on Centrifuge, A A. Balkema Rotterdam, Netherlands 791–796.

Herten, M., M. Pulsfort (1999) Determination of spatial earth pressure on circular shaft constructions. Granular Matter 2(1): 1–7.

Imamura, S., T. Nomoto., T. Fujii., T. Hagiwar (1999) Earth pressures acting on a deep shaft and the movements of adjacent ground in sand. In: Kusakabe, O., Fujita, K., Miyazaki, Y. (Eds.), Proceedings of the International Symposium on Geotechnical Aspects of Underground Construction in Soft Ground. Balkema, Rotterdam, Tokyo, Japan 647–652.

Kim K.Y., D. S. Lee., J. Y. Cho., S. S. Jeong (2013) The effect of arching pressure on a vertical circular shaft., Tunn. Undergr. Space Technol. 37: 10–21.

Liu, F. Q., J. H. Wang., (2008) A generalized slip line solution to the active earth pressure on circular retaining walls. Comput. Geotech. 35 (2): 155–164.

Liu, F. Q., J. H. Wang., L. L. Zhang (2009) Axi-symmetric active earth pressure obtained by the slip line method with a general tangential stress coefficient. Comput. Geotech. 36 (1–2): 352–358.

Prater, E. G. (1977) Examination of some theories of earth pressure on shaft linings. Can. Geotech. J. 14(1): 91–106.

Terzaghi, K. (1943) Theoretical soil mechanics. Wiley, New York.

Tobar, T., M. Meguid (2011) Experimental study of the earth pressure distribution on cylindrical shafts. J. Geotech. Geoenviron. Eng. 137: 1121-1125.

Westergaard, H. M. (1941) Plastic state of stress around deep well. Civ. Eng. , London 36 (421): 527–528.